J. Fluid Mech. (1981), *vol.* 107, *pp.* 147-171
Printed in Great Britain

A semi-analytic solution for nonlinear standing waves in deep water

By L. W. SCHWARTZ†
Applied Mathematics Department, University of Adelaide, Adelaide, South Australia
AND A. K. WHITNEY
Applied Mechanics Laboratory, Lockheed Research Laboratory, Palo Alto, California

(Received 22 February 1980 and in revised form 4 August 1980)

A method of time-dependent conformal mapping is introduced to simplify the power-series solution procedure for time- and space-periodic standing waves in deep water. A solution has been found to 25th order in the wave amplitude. The values of certain coefficients are determined by the requirement that secular terms must be suppressed. Because the series for the wave profile is not always uniformly convergent, Padé approximants are used for summation. For very high waves, the slope of the surface has at least two relative maxima. The singularity structure of the solution is also discussed.

1. Introduction

Standing-gravity-wave problems are more difficult to analyse than those of steady wave motions, such as the classical Stokes progressive wave, because of the complications introduced by their time dependence. Nevertheless, approximate small-amplitude expansions have been found for many cases of interest: two- and three-dimensional waves on a fluid of finite and infinite depth; composite waves of more than one fundamental frequency; interfacial waves in multi-layered fluids; and effects due to surface tension. A survey of these and other standing-wave problems may be found in the review articles of Wehausen & Laitone (1960) and Wehausen (1965).

In the present work we take a fresh look at the most fundamental standing-wave problem: the two-dimensional, simply periodic irrotational motion of a perfect fluid in an infinitely deep and laterally unbounded ocean. In contrast to the progressive-wave case, an existence proof for standing waves has not yet been found. In addition, there remain doubts as to the form of the highest standing-wave profile.

Finite-amplitude deep-water standing waves were first investigated by Rayleigh (1915) who obtained a third-order solution in an assumed small-amplitude expansion. Two important features of deep-water stationary waves become apparent in the first few orders: the maximum elevation of the surface above the mean water level exceeds the maximum depression below it, and the frequency of the wave motion is decreased by an increase in wave amplitude. The latter is not true for shallow water standing waves when the water depth/wavelength ratio is less than 0·17; here the frequency increases with amplitude (Tadjbakhsh & Keller 1960; Fultz 1962).

In the most ambitious effort to date, Penney & Price (1952) carried the perturbation expansion to the fifth order. They found that there is no time during the period of the

† Now at Exxon Research Center, Linden, New Jersey.

wave motion when the free surface is perfectly flat (a fourth-order effect). Even more surprising, they concluded that the crest of the highest wave has a right-angled nodal form in contrast with that of the greatest stable travelling wave, for which the nodal angle is 120°. In showing this, it was necessary to assume, first of all, that the crest is pointed and, secondly, that the pressure is expandable in a Taylor series about the crest. By further arguing that the acceleration of the crest could not exceed g in magnitude, they found a maximum wave-height/length ratio of 0·218 with a corresponding frequency of 0·949 times the frequency of the infinitesimal wave theory. These predictions were later confirmed experimentally by Taylor (1953) who, while he doubted some of the underlying assumptions of Penney & Price's theoretical analysis, nevertheless believed their results to be correct. Experiments by Edge & Walters (1964) also showed a highest wave crest of nearly 90°.

A recent study by Saffman & Yuen (1979) has provided numerical confirmation of Taylor's experimental observations. Their technique computed the time evolution of a given initial state which did not recur exactly after one 'period'. Thus the waves generated are not the 'pure' standing waves discussed here.

In the theoretical studies mentioned above Eulerian co-ordinates were used to describe the fluid motion; i.e. the independent variables are the physical space co-ordinates and time. The feasibility of using a Lagrangian description has been demonstrated by Sekerzh-Zen'kovich (1947), Chabert-D'Hières (1960), and others. In this co-ordinate system, the free surface may be taken to be a straight line, thereby avoiding problems associated with the satisfaction of boundary conditions on free, or unknown, boundaries. One aspect of the Lagrangian method makes it less desirable however: the field equations, i.e. the continuity equation and irrotationality condition, are nonlinear and lead, in practice, to the solution of Poisson's equation at each order in the perturbation expansion. We prefer a third method which is a direct adaptation of the conformal mapping methods described in Whitney (1971) and Grant (1973*b*). Here the flow region in the z plane is mapped conformally to a fixed lower half-plane, say ζ, by a time-dependent mapping $z(\zeta, t)$. Since the Cauchy–Riemann field equations are invariant under a conformal mapping, the problem then becomes one of finding the mapping $z(\zeta, t)$, the complex velocity potential, and the complex velocity, that are analytic functions in ζ under appropriate boundary conditions applied on $\operatorname{Im}\zeta = 0$. In a sense this method combines the best features of the Eulerian and Lagrangian methods.

In the present work we carry the small-amplitude expansion for deep-water standing waves to 25th order, using the computer to perform the laborious arithmetic. Our purpose in doing this is to improve upon the accuracy of previous work and to investigate the nature of limiting singularities. While the solution technique is, by necessity, different, the analysis of the perturbation expansion closely follows the work of Schwartz (1974) who performed a computer extension of Stokes' progressive wave. In § 2, the perturbation solution and recurrence relations are presented and a solution algorithm for them is developed. In § 3, the convergence of the series is analysed; it is analytically continued by Padé fractions; the structure of singularities is determined; and wave profiles and frequencies are calculated.

Preliminary results of the present work (Schwartz & Whitney 1977) were presented at the Sixth Australasian Hydraulics and Fluid Mechanics Conference.

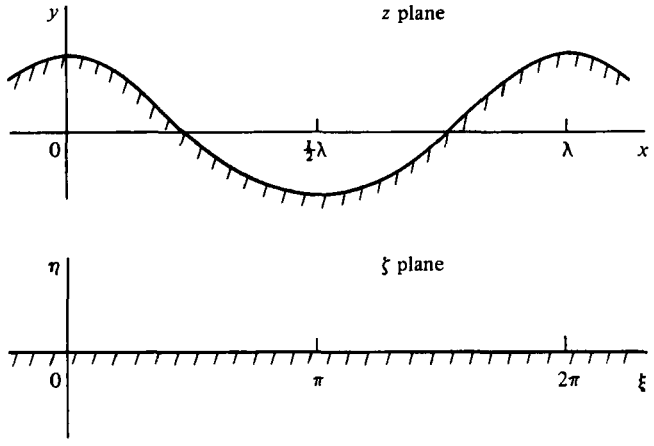

FIGURE 1. One wave cycle in the physical and transformed planes.

2. Formulation

Stokes (1880) showed that the algebraic manipulations in the series solution for the progressive wave can be simplified considerably by treating the complex potential as the independent, rather than the dependent, variable. The free surface is then mapped onto the velocity potential axis and the problem reduces to one that is quadratically, rather than exponentially, nonlinear. We seek a similar simplification for the standing wave.

The region of the physical or z plane occupied by the fluid at each instant of time t is mapped onto the lower half ζ plane according to the transformation

$$z = x + iy = z(\zeta, t; \epsilon), \tag{2.1}$$

where ϵ is a parameter that subsequently will be identified with the wave height and $\zeta = \xi + i\eta$. The free surface corresponds to $\eta = 0$ (see figure 1). We introduce the usual complex velocity potential $f = \phi + i\psi$ and the complex velocity $w = df/dz = u - iv$. Henceforth, capital letters will denote the direct functional dependence of these quantities on ζ and t, i.e.

$$\left.\begin{aligned} F(\zeta, t) &= \Phi + i\Psi \equiv f[z(\zeta, t), t], \\ W(\zeta, t) &= U - iV \equiv w[z(\zeta, t), t]. \end{aligned}\right\} \tag{2.2}$$

The variables W, F and z are related by

$$W = \frac{dF}{dz} = \frac{F_\zeta}{z_\zeta}, \tag{2.3}$$

where subscripts signify partial differentiation.

The kinematic boundary condition states that the normal component of fluid velocity (U, V) of a particle occupying a point on the surface is equal to the normal component of the surface velocity (x_t, y_t) at that point. On the free surface, (x_ξ, y_ξ) is a tangent vector; hence $\mathbf{n} = (-y_\xi, x_\xi)$ is a vector normal to the surface. Thus

$$(U, V).\mathbf{n} = (x_t, y_t).\mathbf{n} \quad \text{on} \quad \eta = 0$$

or, in compact form,

$$\operatorname{Im}\{F_\zeta - z_\zeta \bar{z}_t\} = 0 \quad \text{on} \quad \eta = 0, \tag{2.4}$$

where use has been made of (2.3) and the bar signifies complex conjugation.

The pressure p at any point in the water, in the z plane, is given by the Bernoulli equation

$$(p - p_0)/\rho = -\phi_t - \tfrac{1}{2} w\bar{w} - gy. \tag{2.5}$$

Here ρ is the density, g the acceleration of gravity, and p_0 the atmospheric pressure, which may, without loss of generality, be set equal to zero. On the free surface, the dynamic boundary condition states that $p = p_0$. Thus

$$\phi_t + \tfrac{1}{2} w\bar{w} + gy = 0 \tag{2.6}$$

on the free surface. We require equation (2.6) in terms of ζ-plane variables evaluated on the free surface $\eta = 0$. Only the velocity potential term involves special treatment. From (2.2) we have

$$F_t = f_t + f_z z_t = f_t + w z_t.$$

By substituting the real part of this expression into (2.6), the dynamic boundary condition becomes

$$\Phi_t + \tfrac{1}{2} W\overline{W} + gy - \operatorname{Re}\{W z_t\} = 0 \quad \text{on} \quad \eta = 0. \tag{2.7}$$

Additional details of this transformation may be found in the paper by Whitney (1971). A similar mapping was used by Grant (1973*b*).

Proceeding now to dimensionless variables, we choose as a characteristic length the wavelength λ and as a characteristic time the unknown period T. Let

$$k = 2\pi/\lambda \quad \text{and} \quad \omega = 2\pi/T$$

be the wavenumber and frequency for the standing-wave motion. We define the dimensionless variables

$$\tilde{z} = kz, \quad \tilde{t} = \omega t, \quad \tilde{F} = \frac{k^2}{\omega} F, \quad \tilde{W} = \frac{k}{\omega} W. \tag{2.8}$$

We make the substitutions indicated by (2.8) in (2.3) and the surface conditions (2.4) and (2.7). After dropping the tildes, (2.3) and (2.4) remain unchanged while (2.7) becomes

$$\Phi_t + \tfrac{1}{2} W\overline{W} + Sy - \operatorname{Re}\{W z_t\} = 0 \quad \text{on} \quad \eta = 0, \tag{2.9}$$

where the frequency parameter S is defined as

$$S = gk/\omega^2. \tag{2.10}$$

If the wavenumber k is considered to be fixed, then the frequency ω, and hence S, will have to be determined as one of the unknowns of the problem.

The dependent functions z, F, and W are required to be analytic in ζ and t in the lower half-plane. The depth of the water is assumed to be infinite; consequently we require

$$z \sim \zeta, \quad W \sim 0 \quad \text{as} \quad \eta \to -\infty \tag{2.11}$$

to ensure that the disturbances vanish far beneath the surface. The analytic and periodic requirements, together with (2.11), imply that the functions may be represented by Fourier series of the form

$$z = \zeta + i \sum_{p=0}^{\infty} a_p e^{-ip\zeta}, \tag{2.12a}$$

$$W = i \sum_{p=0}^{\infty} b_p e^{-ip\zeta}, \tag{2.12b}$$

$$F = \sum_{p=0}^{\infty} c_p e^{-ip\zeta}, \tag{2.12c}$$

where we have chosen the η axis to be a line of symmetry. Inserting the expansions (2.12) into (2.3) and setting coefficients of each harmonic equal to zero readily yields $b_0 = 0$ and

$$b_p + pc_p + \sum_{j=1}^{p-1} j a_j b_{p-j} = 0, \quad p = 1, 2, \ldots. \tag{2.13}$$

Here we introduce the convention that sums where the lower limit exceeds the upper are taken to be identically equal to zero. Similarly, the kinematic surface condition becomes

$$a_p' - pc_p + H_p \sum_{j=0}^{\infty} [j a_j a_{p+j}' + (p+j) a_{p+j} a_j'] = 0, \quad p = 0, 1, 2, \ldots, \tag{2.14}$$

where the factor H_p is defined by

$$H_p = \begin{cases} \frac{1}{2} & \text{if} \quad p = 0 \\ 1 & \text{if} \quad p > 0 \end{cases}$$

and the primes signify time differentiation. Finally, the dynamic condition gives

$$c_p' + S a_p + H_p \sum_{j=1}^{\infty} b_j b_{p+j} + \sum_{j=1}^{p} b_j a_{p-j}' = 0, \quad p = 0, 1, \ldots. \tag{2.15}$$

The required solution has the property that when ϵ, the wave height, is very small the surface profile is simply periodic in space and time with frequency and wavenumber both equal to 2π. That is

$$y = \epsilon \cos x \cos t + O(\epsilon^2), \tag{2.16}$$

where analytic dependence on ϵ is also assumed and we have arbitrarily specified that $x = 0$ corresponds to a crest when $t = 0$. Equation (2.16) is compatible with (2.12a) only if a_1 is $O(\epsilon)$ and all other a_p are $o(\epsilon)$. The quadratic sums in (2.13)–(2.15) are all $O(\epsilon^2)$; consequently b_1 and c_1 are also $O(\epsilon)$. Finally, combining (2.14) and (2.15) with $p = 1$ shows that S must be 1 to leading order. Calculation of the first few orders in an assumed ϵ expansion quickly reveals that it is sufficient to assume a Stokes-type expansion; that is

$$a_p = \sum_{n=0}^{\infty} \alpha_{pn} \epsilon^{p+2n}, \tag{2.17a}$$

$$b_p = \sum_{n=0}^{\infty} \beta_{pn} \epsilon^{p+2n}, \tag{2.17b}$$

$$c_p = \sum_{n=0}^{\infty} \gamma_{pn} \epsilon^{p+2n}, \tag{2.17c}$$

and

$$S = 1 + \sum_{n=1}^{\infty} \sigma_n \epsilon^{2n}. \tag{2.17d}$$

Here σ_n are constants to be determined and the doubly subscripted elements are periodic functions of t. Note that α_{00}, γ_{00}, and β_{0n} are all zero.

Introducing the expansions (2.17) into the system (2.13)–(2.15) and equating coefficients of each power of ϵ, we obtain

$$\beta_{pn} + p\gamma_{pn} = -\sum_{k=0}^{n} \sum_{j=1}^{p-1} j\alpha_{jk}\beta_{p-j,n-k}, \tag{2.18a}$$

$$\alpha'_{pn} - p\gamma_{pn} = -H_p \sum_{k=0}^{n} \sum_{j=0}^{n-k} [k\alpha_{k,n-k-j}\alpha'_{p+k,j} + (p+k)\alpha_{p+k,n-k-j}\alpha'_{kj}], \tag{2.18b}$$

$$\gamma'_{pn} + \alpha_{pn} = -\sum_{k=0}^{n-1} \sigma_{n-k}\alpha_{pk} - \sum_{k=0}^{n} \left[H_p \sum_{j=0}^{n-k} \beta_{kj}\beta_{p+k,n-k-j} + \sum_{j=0}^{p-1} \alpha'_{j,n-k}\beta_{p-j,k} \right]. \tag{2.18c}$$

Here p and n assume non-negative integer values. The elements on the left-hand sides of (2.18) are all $O(\epsilon^{p+2n})$, while the right-hand sides consist of sums of products of coefficients of lower order. These equations are quite similar to an analogous set for the progressive wave as given by Schwartz (1974); however, there the recurrence relations were purely algebraic. Equations (2.18), on the other hand, contain time derivatives and a special treatment will be required for the suppression of secular terms.

A recursive calculation soon reveals the nature of the time dependence. Consistently with (2.16) we set the first-order solution

$$\alpha_{10} = \cos t.$$

Now equations (2.18) with $p = 1$ and $n = 0$ give

$$\beta_{10} = \sin t, \quad \gamma_{10} = -\sin t.$$

We assume that the surface profile and hence the function z is an even function of time. From (2.3) and (2.4) it then follows that W and F are odd functions. Proceeding to second order in ϵ, we find that, with $p = 0$ and $n = 1$ in (2.18),

$$\alpha_{01} = -\tfrac{1}{4}(1 + \cos 2t),$$

and

$$\gamma_{01} = \tfrac{1}{4} \sin 2t.$$

Let $R^{(1)}_{pn}$, $R^{(2)}_{pn}$, and $R^{(3)}_{pn}$ represent the right-hand sides of (2.18a), (2.18b), and (2.18c), respectively. A single non-homogeneous 'spring' equation can be found for α_{pn} by differentiating (2.18b) and adding (2.18c). One obtains

$$\alpha''_{pn} + p\alpha_{pn} = R^{(2)}_{pn} + pR^{(3)}_{pn}. \tag{2.19}$$

A particular solution to (2.19) with $p = 2$ and $n = 0$ is

$$\alpha_{20} = \tfrac{1}{2}(1 + \cos 2t).$$

A homogeneous solution is not permitted because its frequency would be an irrational multiple of the fundamental and thus would violate the periodicity requirement.

Corresponding expressions for γ_{20} and β_{20} can be obtained from (2.18*b*) and (2.18*a*). These are

$$\gamma_{20} = -\tfrac{1}{2}\sin 2t, \quad \beta_{20} = \tfrac{1}{2}\sin 2t.$$

In general, a sufficient assumption for the form of the coefficient is

$$\alpha_{pn} = \sum_{l=0}^{[\frac{1}{2}(2n+p)]} \alpha_{pnl}\cos(p+2n-2l)\,t, \tag{2.20a}$$

$$\beta_{pn} = \sum_{l=0}^{[\frac{1}{2}(2n+p-1)]} \beta_{pnl}\sin(p+2n-2l)\,t, \tag{2.20b}$$

and

$$\gamma_{pn} = \sum_{l=0}^{[\frac{1}{2}(2n+p-1)]} \gamma_{pnl}\sin(p+2n-2l)\,t. \tag{2.20c}$$

The square brackets are used here to signify the integer-part function. These forms may be inserted on the right-hand sides of the system (2.18). After multiplying cosine harmonics and sorting, we obtain

$$R^{(1)}_{pn} = \sum_{l=0}^{[\frac{1}{2}(2n+p-1)]} R^{(1)}_{pnl}\sin(p+2n-2l)\,t, \tag{2.21a}$$

$$R^{(2)}_{pn} = \sum_{l=0}^{[\frac{1}{2}(2n+p-1)]} R^{(2)}_{pnl}\sin(p+2n-2l)\,t, \tag{2.21b}$$

$$R^{(3)}_{pn} = \sum_{l=0}^{[\frac{1}{2}(2n+p)]} R^{(3)}_{pnl}\cos(p+2n-2l)\,t. \tag{2.21c}$$

We have not obtained explicit forms for the $R^{(j)}_{pnl}$; fortunately they are not needed. All that we require is an *algorithm* for assigning values to these constants. For example, the right-hand side of (2.18*a*) becomes

$$\sum_{j=1}^{p-1}\sum_{k=0}^{n}\sum_{r=0}^{[\frac{1}{2}(2k+j)]}\sum_{m=0}^{[\frac{1}{2}(2n-2k+p-j-1)]} K(\alpha,\beta)\,[\sin(q_1+q_2)\,t+\sin(q_1-q_2)\,t],$$

where

$$q_1 = p-j+2n-2k-2m, \quad q_2 = j+2k-2r,$$

and

$$K(\alpha,\beta) = -\frac{j}{2}\alpha_{jkr}\beta_{p-j,\,n-k,\,m}.$$

The quadruple sum is performed with the current value of K being added to $R^{(2)}_{pnl}$, where $l = m+r$. Finally the sum is repeated with K being either added to, or subtracted from, $R^{(1)}_{pnl}$, $l = |p+2n-2q_1+2q_2|$, according to whether (q_1-q_2) is positive or negative.

Once the triply subscripted elements in (2.21) have been determined, substitution of (2.20) and (2.21) into (2.19) yields an expression

$$[p-(p+2n-2l)^2]\,\alpha_{pnl} = (p+2n-2l)\,R^{(2)}_{pnl}+R^{(3)}_{pnl}, \tag{2.22}$$

from which α_{pnl} is uniquely determined provided, of course, that $p \neq (p+2n-2l)^2$. γ_{pnl} and β_{pnl} can then be found from the algebraic equations (2.18*a*) and (2.18*b*).

The restriction on equation (2.22) can be violated when p is a perfect square; that

is for $p = 0, 1, 4, 9, \ldots$. We will consider each case in turn. For $p = 0$ and $n = 1$, $\gamma_{0nn} = \alpha'_{0nn} = 0$ and α_{0nn} is found from (2.18c) algebraically:

$$\alpha_{0nn} = R^{(3)}_{0nn}.$$

When $p = 1$ and $n = 1$, terms containing $t\cos t$ will appear unless

$$R^{(2)}_{1nn} + R^{(3)}_{1nn} = 0. \tag{2.23}$$

These secular terms are unacceptable because they would violate the time-periodicity requirement on the solution. Inspection of the right side of (2.18c) reveals that $R^{(3)}_{1n}$ contains a term

$$\sigma_n \alpha_{10} = \sigma_n \cos t.$$

The constant σ_n does not appear in the equations for any other quantity of $O(\epsilon^{2n+1})$, nor is it required at lower order. Thus σ_n may be determined at this point by satisfying condition (2.23).

The homogeneous solution $\alpha_{1nn}\cos t$ is still undetermined. Its determination is equivalent to the specification of the expansion parameter ϵ. We choose ϵ to be equal to half the (dimensionless) peak-to-trough wave height at $t = 0$. Thus, if $y(\xi, t)$ gives the vertical co-ordinate of a point on the surface, the crest displacement is

$$y(0,0) = \sum_{p=0}^{\infty} \sum_{n=0}^{\infty} \sum_{k=0}^{[\frac{1}{2}(2n+p)]} \epsilon^{p+2n} \alpha_{pnk}.$$

The y co-ordinate of a trough is

$$y(\pi, 0) = y(0, \pi) = \sum_{p=0}^{\infty} \sum_{n=0}^{\infty} \sum_{k=0}^{[\frac{1}{2}(2n+p)]} (-1)^p \epsilon^{p+2n} \alpha_{pnk}.$$

But $2\epsilon = y(0,0) - y(\pi, 0)$, from which it follows that

$$\alpha_{100} = 1$$

and

$$\sum_{l=0}^{n} \sum_{k=0}^{n} \alpha_{1+2n-2l,\,l,\,k} = 0 \quad n = 1, 2, \ldots. \tag{2.24}$$

Equation (2.24) determines the value of α_{1nn} once all the other α's of order ϵ^{2n+1} are known.

The system (2.18) appears to indicate that α_{pn}, β_{pn}, and γ_{pn} can be calculated only from elements whose second subscript, r say, is less than or equal to n; however, this is not true in general. Let us consider the first 'resonant' term that appears when $p = 4$. The element α_{40} contains the term

$$\alpha_{401}\cos 2t$$

for which $p = (p + 2n - 2l)^2$ in the notation of equation (2.22). We first verify that $2R^{(2)}_{401} + 4R^{(3)}_{401}$ is indeed zero so that no secular term appears at fourth order. If we take α_{401} to be equal to zero we soon find that resonance occurs at order ϵ^6 because $2R^{(2)}_{412} + 4R^{(3)}_{412}$ is not zero. We can, however, select α_{401} so as to induce a zero value at $(p, n, l) = (4, 1, 2)$. Similarly, the homogeneous term α_{412} is selected to suppress the secular term at (4, 2, 3). The next homogeneous term with $p = 4$ is α_{423}. Its determination requires suppression of resonance at (4, 3, 4). This last node, however, is $O(\epsilon^{10})$; this calculation therefore requires knowledge of α_{903}, whose value is specified so as to suppress resonance at (9, 1, 4).

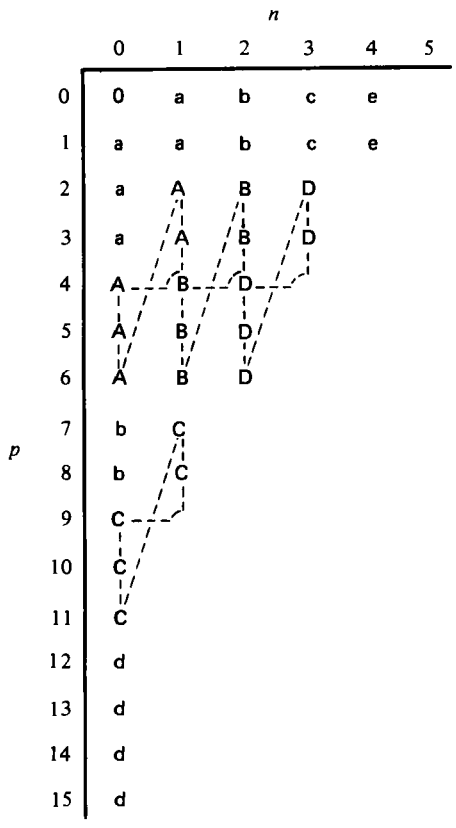

FIGURE 2. Order of procedure scheme for a ninth-order solution.

This process, which may be continued indefinitely, is illustrated schematically in figure 2. The coefficient with (p, n) values whose nodes contain the same symbol in the figure are to be calculated as outlined above in order of increasing total order, $p+2n$. The overall progression is in the order

$$\mathsf{aAbBcCdDe....}$$

The dotted lines and capital letters indicate resonance-suppression loops.

A careful examination of the recurrence relations reveals a linear relation between the right-hand side of (2.22) and the preceding homogeneous coefficient

$$p^{\frac{1}{2}}R^{(2)}_{pnl} + pR^{(3)}_{pnl} = K_{pnl} + \tfrac{1}{4}p\alpha_{p,n-1,l-1},$$

where $(p+2n-2l)^2 = p$. Thus only two passes through each loop are necessary: the first to determine the value of K_{pnl}; and the second to find final values for the coefficient.

Any secular term for $n > 0$ can be suppressed by this procedure. If, on the other hand, a secular term were to appear for $n = 0$, i.e. in the first column in figure 2, it could not be removed for there are no additional disposable constants in the solution. This would be quite serious since it would either invalidate the representation used here or cast doubt on the existence of a time- and space-periodic standing wave. We

have been unable to prove that secular terms will not appear in the first column but we can offer strong numerical evidence that they will not.

The recurrence equations (2.18) with $n = 0$ completely determine α_{n0}, β_{n0}, and γ_{n0}, once the homogeneous constants $\alpha_{100}, \alpha_{401}, \alpha_{903}, \ldots$ are specified. A first-column computation was run to $O(\epsilon^{81})$ with *randomly selected* real values for these constants. The right-hand side of (2.22) was found to be zero to double-precision accuracy for all possible resonance cases; i.e. at $p = 4, 9, 16, \ldots, 81$ and $l = \frac{1}{2}(p - p^{\frac{1}{2}})$. The first-column computation is further discussed in the appendix.

3. Discussion of results

The algorithm described in the preceding section has been coded in FORTRAN and run to $O(\epsilon^{25})$ on a CDC 6400 computer. Double-precision results (29 significant figures) for the three arrays α_{pnl}, β_{pnl}, and γ_{pnl} required a run time of about 4 minutes. The time required for a run of given total order M was roughly proportional to M^6.

Through order ϵ^5, the series coefficients can be recognized as rational numbers from their decimal expansions. The coefficients a_p in the transformation equation (2.12a) are

$$\left.\begin{aligned}
a_0 &= -\tfrac{1}{4}\epsilon^2 + \tfrac{13}{64}\epsilon^4 - (\tfrac{1}{4}\epsilon^2 - \tfrac{1}{4}\epsilon^4)\cos 2t + \tfrac{3}{64}\epsilon^4 \cos 4t,\\
a_1 &= (\epsilon - \tfrac{37}{32}\epsilon^3 + \tfrac{1324607}{788448}\epsilon^5)\cos t + (-\tfrac{11}{32}\epsilon^3 + \tfrac{15016}{17952}\epsilon^5)\cos 3t + \tfrac{9155}{71168}\epsilon^5 \cos 5t,\\
a_2 &= \tfrac{1}{2}\epsilon^2 - \tfrac{39}{32}\epsilon^4 + (\tfrac{1}{2}\epsilon^2 - \tfrac{7}{4}\epsilon^4)\cos 2t - \tfrac{87}{224}\epsilon^4 \cos 4t,\\
a_3 &= (\tfrac{9}{8}\epsilon^3 - \tfrac{1883}{384}\epsilon^5)\cos t + (\tfrac{3}{8}\epsilon^3 - \tfrac{46499}{17952}\epsilon^5)\cos 3t - \tfrac{2719193}{5913136}\epsilon^5 \cos 5t,\\
a_4 &= \epsilon^4 + \tfrac{65}{48}\epsilon^4 \cos 2t + \tfrac{1}{8}\epsilon^4 \cos 4t,\\
a_5 &= \tfrac{635}{1952}\epsilon^5 \cos t + \tfrac{2155}{1288}\epsilon^5 \cos 3t + \tfrac{1255}{3884}\epsilon^5 \cos 5t.
\end{aligned}\right\} \tag{3.1}$$

The frequency parameter has the expansion

$$\begin{aligned}
S = \frac{gk}{\omega^2} = 1 &+ \tfrac{1}{4}\epsilon^2 - \tfrac{5}{128}\epsilon^4 - \tfrac{18255}{118272}\epsilon^6 - 0{\cdot}010839\epsilon^8 - 0{\cdot}063683\epsilon^{10} - 0{\cdot}134050\epsilon^{12}\\
&- 0{\cdot}238688\epsilon^{14} - 0{\cdot}532647\epsilon^{16} - 1{\cdot}24212\epsilon^{18} - 2{\cdot}72405\epsilon^{20} - 6{\cdot}00315\epsilon^{22}\\
&- 13{\cdot}7416\epsilon^{24} - \ldots.
\end{aligned} \tag{3.2}$$

From (3.1) we can immediately draw an important conclusion: there is no instant of time at which the free surface is perfectly flat. It is most nearly flat at $t = \frac{1}{2}\pi \pm n\pi$, $n = 1, 2, \ldots$. At these values of t (2.12a) becomes

$$z = \zeta + i\epsilon^4(\tfrac{1}{7}e^{-2i\zeta} - \tfrac{1}{48}e^{-4i\zeta}) + O(\epsilon^6),$$

which, on the free surface $\zeta = \xi$, gives immediately

$$y = \epsilon^4(\tfrac{1}{7}\cos 2x - \tfrac{1}{48}\cos 4x) + O(\epsilon^6). \tag{3.3}$$

Penney & Price (1952) have previously determined that the surface is never flat and therefore concluded 'that strictly periodic oscillations of finite amplitude cannot be generated by impulsive pressures applied to the initially flat surface of water at rest'. Their solution corresponding to (3.3) would seem to be incorrect; in particular, while their result gave $\frac{1}{7}$ as the coefficient of $\cos 2x$ in (3.3), the $\cos 4x$ term was absent. This error was undoubtedly caused by the improper choice of a homogeneous term

	n										
p	0	1	2	3	4	5	6	7	8	9	10
0	0	-5.000×10^{-1}	$5\cdot000\times10^{-1}$	$-4\cdot310\times10^{-1}$	$1\cdot560\times10^{-1}$	$2\cdot668\times10^{-1}$	$-1\cdot515\times10^{-2}$	$1\cdot193\times10^{-1}$	$8\cdot735\times10^{-1}$	1·586	2·853
1	1·000	−1·500	2·645	−3·579	3·362	−2·454	1·145	−1·708	$5\cdot095\times10^{-2}$	−2·948	−6·001
2	1·000	−3·357	8·743	$-1\cdot736\times10$	$2\cdot796\times10$	$-3\cdot740\times10$	$4\cdot410\times10$	$-4\cdot548\times10$	$4\cdot519\times10$	$-3\cdot647\times10$	
3	1·500	−7·958	$2\cdot765\times10$	$-7\cdot315\times10$	$1\cdot575\times10^{2}$	$-2\cdot885\times10^{2}$	$4\cdot605\times10^{2}$	$-6\cdot570\times10^{2}$	$8\cdot444\times10^{2}$	$-1\cdot003\times10^{3}$	
4	2·688	$-1\cdot945\times10$	$8\cdot534\times10$	$-2\cdot806\times10^{2}$	$7\cdot492\times10^{2}$	$-1\cdot701\times10^{3}$	$3\cdot374\times10^{3}$	$-5\cdot975\times10^{3}$	$9\cdot567\times10^{3}$		
5	5·313	$-4\cdot860\times10$	$2\cdot585\times10^{2}$	$-1\cdot015\times10^{3}$	$3\cdot218\times10^{3}$	$-8\cdot652\times10^{3}$	$2\cdot032\times10^{4}$	$-4\cdot258\times10^{4}$	$8\cdot075\times10^{4}$		
6	$1\cdot117\times10$	$-1\cdot235\times10^{2}$	$7\cdot725\times10^{2}$	$-3\cdot523\times10^{3}$	$1\cdot290\times10^{4}$	$-3\cdot996\times10^{4}$	$1\cdot079\times10^{5}$	$-2\cdot598\times10^{5}$			
7	$2\cdot453\times10$	$-3\cdot176\times10^{2}$	$2\cdot285\times10^{3}$	$-1\cdot187\times10^{4}$	$4\cdot925\times10^{4}$	$-1\cdot722\times10^{5}$	$5\cdot243\times10^{5}$	$-1\cdot421\times10^{6}$			
8	$5\cdot557\times10$	$-8\cdot245\times10^{2}$	$6\cdot706\times10^{3}$	$-3\cdot908\times10^{4}$	$1\cdot811\times10^{5}$	$-7\cdot047\times10^{5}$	$2\cdot383\times10^{6}$				
9	$1\cdot289\times10^{2}$	$-2\cdot156\times10^{3}$	$1\cdot956\times10^{4}$	$-1\cdot264\times10^{5}$	$6\cdot462\times10^{5}$	$-2\cdot768\times10^{6}$	$1\cdot029\times10^{7}$				
10	$3\cdot046\times10^{2}$	$-3\cdot670\times10^{3}$	$5\cdot678\times10^{4}$	$-4\cdot026\times10^{5}$	$2\cdot252\times10^{6}$	$-1\cdot052\times10^{7}$					
11	$7\cdot309\times10^{2}$	$-1\cdot498\times10^{4}$	$1\cdot642\times10^{5}$	$-1\cdot267\times10^{6}$	$7\cdot694\times10^{6}$	$-3\cdot894\times10^{7}$					
12	$1\cdot776\times10^{3}$	$-3\cdot975\times10^{4}$	$4\cdot729\times10^{5}$	$-3\cdot949\times10^{6}$	$2\cdot586\times10^{7}$						
13	$4\cdot359\times10^{3}$	$-1\cdot058\times10^{5}$	$1\cdot358\times10^{6}$	$-1\cdot220\times10^{7}$	$8\cdot568\times10^{7}$						
14	$1\cdot080\times10^{4}$	$-2\cdot824\times10^{5}$	$3\cdot892\times10^{6}$	$-3\cdot740\times10^{7}$							
15	$2\cdot695\times10^{4}$	$-7\cdot558\times10^{5}$	$1\cdot113\times10^{7}$	$-1\cdot139\times10^{8}$							
16	$6\cdot773\times10^{4}$	$-2\cdot027\times10^{6}$	$3\cdot174\times10^{7}$								
17	$1\cdot712\times10^{5}$	$-5\cdot446\times10^{6}$	$9\cdot042\times10^{7}$								
18	$4\cdot350\times10^{5}$	$-1\cdot466\times10^{7}$									
19	$1\cdot110\times10^{6}$	$-3\cdot951\times10^{7}$									
20	$2\cdot846\times10^{6}$										
21	$7\cdot323\times10^{6}$										

TABLE 1. Transformation coefficients α_{pn} for time $t = 0$.

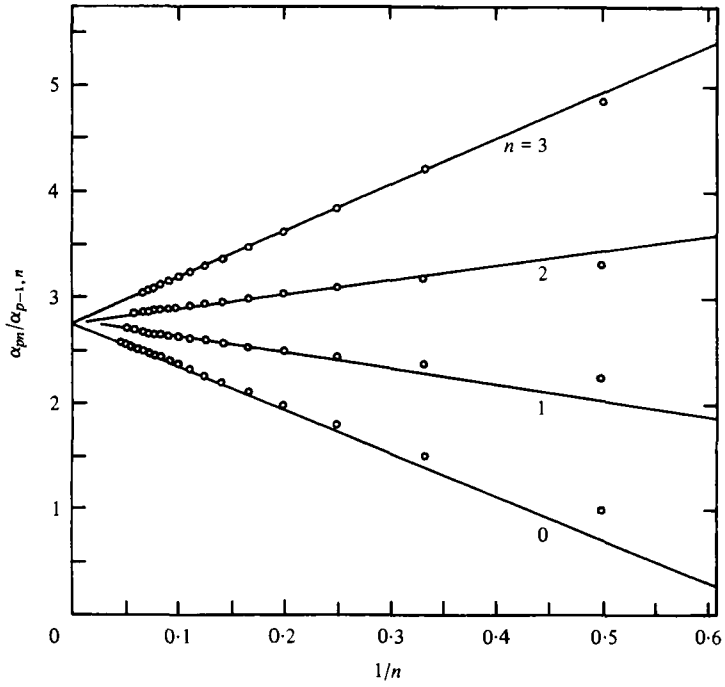

FIGURE 3. Domb–Sykes plots for $\alpha_{pn}/\alpha_{p-1,n}$ at $t = 0$.

at the fourth order which gives rise to a secular term at $O(\epsilon^6)$ (see § 2). Since their solution was only carried to $O(\epsilon^5)$, they were not aware of this fact.

The total number of transformation coefficients α_{pnl} for a twenty-fifth order solution is 1637, far too many to be presented meaningfully. By way of compromise, and since the highest wave profile ($t = 0$) for a given value of ϵ is of particular interest, we show the coefficients $\alpha_{pn}(0)$ to $O(\epsilon^{21})$ in table 1.

A useful tool for extracting information from a high-order series computation is a graphical ratio test used by Domb & Sykes (1957). It is based on the observation that, if f is a binomial function,

$$f(\epsilon) = \sum_{n=0}^{\infty} a_n \epsilon^n = \begin{cases} (\epsilon^* - \epsilon)^\alpha & \text{if} \quad \alpha \neq 0, 1, \ldots, \\ (\epsilon^* - \epsilon)\ln(\epsilon^* - \epsilon) & \text{if} \quad \alpha = 0, 1, \ldots, \end{cases} \tag{3.4a}$$

then

$$\frac{a_n}{a_{n-1}} = \frac{1}{\epsilon^*}\left[1 - \frac{1+\alpha}{n}\right] \tag{3.4b}$$

is an exact relation. If an arbitrary function $F(\epsilon)$, analytic at $\epsilon = 0$, possesses a singularity at ϵ^* of the type (3.4a) and if the singularity is closer to the origin than any other singularity of F, then a plot of the ratio of expansion coefficients *versus* $1/n$ will possess a straight-line asymptote as indicated by (3.4b). It has not generally been realized that (3.4) is valid for complex values of a_n, in which case the asymptote will be a straight line in $(1/n, \mathrm{Re}\{a_n/a_{n-1}\}, \mathrm{Im}\{a_n/a_{n-1}\})$ space. When a large but finite number of coefficients are known in a series expansion, the location ϵ^* and nature α of the limiting singularity can often be found to good accuracy by this graphical method.

Typical Domb–Sykes plots formed from subsequences in table 1 are shown in figure 3. From (2.12a) and (2.17a), the transformation expansion at $t = 0$ can be written as

$$z = \zeta + i\{\sum_{p=0} \alpha_{p0}(e^{-i\zeta}\epsilon)^p + \epsilon^2 \sum_{p=0} \alpha_{p1}(e^{-i\zeta}\epsilon)^p + \epsilon^4 \sum_{p=0} \alpha_{p2}(e^{-i\zeta}\epsilon)^p + \ldots\}. \tag{3.5}$$

The coefficient ratios corresponding to vertical columns in table 1, $(\alpha_{p0}/\alpha_{p-1,0})$, $(\alpha_{p1}/\alpha_{p-1,1})$, $(\alpha_{p2}/\alpha_{p-1,2})$, and $(\alpha_{p3}/\alpha_{p-1,3})$, when plotted versus $1/p$ give the 'curves' shown in the figure. For each set of ratios, the points clearly indicate straight-line asymptotes with a vertical intercept, $1/K^*$ say, of about 2·77. The slopes indicate approximate α values of 0·50, $-0{\cdot}46$, $-1{\cdot}49$, $-2{\cdot}57$, respectively. In general, α cannot be estimated as accurately as K^*; it is quite plausible therefore to assume that the α's should properly be half-integers. Therefore, for $|\epsilon e^{-i\zeta} - K^*| \ll 1$, (3.5) can be replaced by

$$z \sim R_1(\zeta, \epsilon)(K^* - \epsilon e^{-i\zeta})^{\frac{1}{2}}\left[A_0 + \frac{\epsilon^2 A_1}{(K^* - \epsilon e^{-i\zeta})} + \frac{\epsilon^4 A_2}{(K^* - \epsilon e^{-i\zeta})^2} + \ldots\right], \tag{3.6}$$

where R_1 is a regular function near the singular point and the A's are constants. Thus the function z appears to have an essential singularity at $\epsilon e^{-i\zeta} = K^* = 0{\cdot}361$. If, on the other hand, we assume, following Grant (1973b), that the wave profile can be approximated in some sense by the first column of table 1, we would expect merely the square root singularity. Interestingly, the value of K^* which we obtain differs little from Grant's value, $e^{-1} = 0{\cdot}368$. Both the value e^{-1} and the square-root behaviour can be obtained from his result $\alpha_{p0}(0) = p^{p-1}/p!$ by considering the limit $p \to \infty$ (see appendix). Assuming that the square-root behaviour is correct, it is easy to show that the wave profile $z(\xi, 0)$ would have a 90° crest at $\xi = 0$ when $\epsilon = K^*$.

Actually neither the square-root behaviour nor the essential singularity is correct, and $\epsilon e^{-i\zeta} = K^*$ is, in fact, a regular point. By considering the last numbers in each of the first few columns, we can show that the quantity in brackets in (3.6) is a square-root expansion as well. Let this quantity be

$$g(\delta) = A_0 + A_1\delta + A_2\delta^2 + \ldots,$$

where $\delta = \epsilon^2/(K^* - \epsilon e^{-i\zeta})$. If we assume that $g(\delta)$ is a binomial function of the type (3.4a), it follows that its singularity exponent α is given by

$$\alpha = \frac{(k^2-1)A_{k+1}/A_k - k^2 A_k/A_{k-1}}{(k+1)A_{k+1}/A_k - kA_k/A_{k-1}}, \quad k = 1, 2, \ldots. \tag{3.7}$$

For sufficiently large p, the coefficients in table 1 can be accurately estimated from the expansions of the 'model' functions suggested by the Domb–Sykes plots of figure 4. Let

$$d_p = (1 - \chi/K^*)^{\frac{1}{2}-p} = \sum_{k=0} d_p^{(k)} \chi^k, \quad p = 0, 1, 2, \ldots, \tag{3.8}$$

denote these model functions where $\chi = \epsilon e^{-i\zeta}$. Thus

$$\alpha_{pk} \simeq A_k d_p^{(k)}$$

should be approximately true for large p. From (3.8) we obtain

$$\frac{A_k}{A_{k-1}} = \frac{\alpha_{pk}}{\alpha_{p+1,k-1}} \frac{d_{p+1}^{(k-1)}}{d_p^{(k)}} = \frac{\alpha_{pk}}{\alpha_{p+1,k-1}} \frac{(2k-3)}{2(p+1)K^*}, \quad k = 1, 2, \ldots.$$

n	x_n	y_n	Re $\{z_n/z_{n-1}\}$	Im $\{z_n/z_{n-1}\}$
0	0·3242	0·0	—	—
1	0·3185	0·9499	0·9826	2·924
2	0·6038	0·2971	0·4740	−0·4778
3	0·7617	−0·5770	0·6370	−1·269
4	0·5599	−1·448	1·382	−0·8544
5	−0·4270	−2·240	1·246	−0·7767
6	−3·038	−2·811	1·460	−1·078
7	−8·046	−1·164	1·618	−1·114
8	−14·31	7·136	1·617	−1·121
9	−15·80	27·61	1·654	−1·104
10	5·565	64·80	1·681	−1·164
11	85·77	104·0	1·705	−1·177
12	272·8	78·10	1·735	−1·192
13	570·8	−192·5	1·747	−1·206
14	774·2	−1033	1·766	−1·215
15	109·5	−2789	1·779	−1·227
16	−3244	−5128	1·790	−1·233
17	−12210	−5213	1·802	−1·241
18	−28610	5803	1·810	−1·248
19	−44750	46420	1·819	−1·254
20	−23230	14110	1·826	−1·260
21	135800	288000	1·833	−1·264

TABLE 2. Coefficients z_n and ratios z_n/z_{n-1} for $\xi = 0{\cdot}3242$ and $t = 0$.

This ratio may be computed most accurately using the largest values of p for which we know α_{pk}. From (3.7) we obtain, for $k = 1$ and 2, the estimate $\alpha = 0{\cdot}50$ and $0{\cdot}49$, respectively, which strongly suggests that $g(\delta)$ is of the form $R_2(C-\delta)^{\frac{1}{2}}$ where R_2 is regular and C is a constant. Thus (3.6) becomes

$$z \sim R_3(K^* - \epsilon e^{-i\zeta})^{\frac{1}{2}}\left[C - \frac{\epsilon^2}{K^* - \epsilon e^{-i\zeta}}\right]^{\frac{1}{2}} \sim R_4(\epsilon, \zeta)$$

for $|K^* - \epsilon e^{-i\zeta}| \ll 1$, where R_3 and R_4 are also regular functions. We conclude that $z(\zeta, 0; \epsilon)$ is regular near the point in question, that the apparent singularity arises because of the particular summation method used, and that any conclusion drawn on the basis of the spurious singularity must be discounted.

Equations (2.12) should properly be considered to be expansions in the parameter ϵ with coefficients which are known polynomials in $e^{-i\zeta}$ and $\begin{Bmatrix}\cos t\\ \sin t\end{Bmatrix}$. Thus, for example, we consider the expansion in the form

$$z(\zeta, t; \epsilon) = \sum_{n=0}^{\infty} z_n(\zeta, t)\,\epsilon^n. \tag{3.9}$$

In table 2 we present the coefficients z_n to $O(\epsilon^{21})$ for a point on the surface corresponding to $\xi = 0{\cdot}3242$ at $t = 0$. The first two columns contain the values x_n and y_n, the real and imaginary parts of z_n. We notice that neither column exhibits much regularity of structure, except that the coefficients increase in magnitude with order and have sign changes about every fifth term. Thus a ratio plot of, say,

$$x = \Sigma x_n \epsilon^n$$

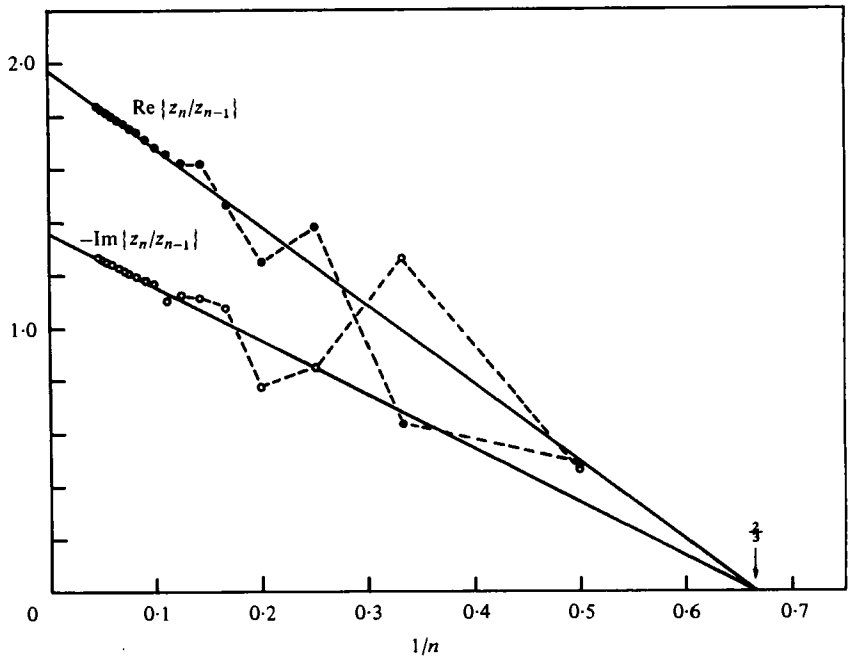

FIGURE 4. Plot of coefficient ratios Re $\{z_n/z_{n-1}\}$ and Im $\{z_n/z_{n-1}\}$ *versus* $1/n$ for $\xi = 0{\cdot}3242$, $t = 0$.

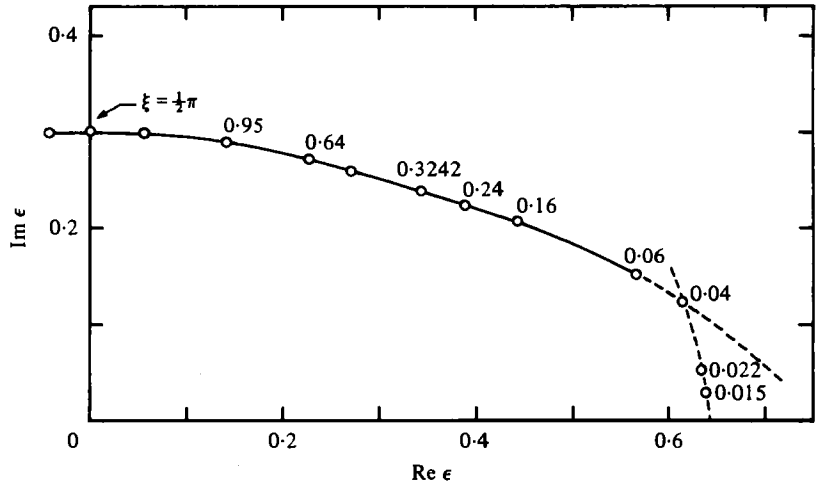

FIGURE 5. Locus of $\epsilon^*(\xi)$, the limiting singularities, for $t = 0$.

would reveal nothing about the structure of z. The result is quite different, however, if we consider the ratio of the complex coefficients. The third and final columns of table 2 contain the values of Re $\{z_n/z_{n-1}\}$ and Im $\{z_n/z_{n-1}\}$. A great deal of structure is apparent past $n \simeq 10$.

Figure 4 is a graph of the coefficient ratios versus n^{-1}. It shows, in effect, the projections of the three-dimensional graph on the planes $(1/n, \mathrm{Re}\{z_n/z_{n-1}\}, 0)$ and

$(1/n, 0, \mathrm{Im}\{z_n/z_{n-1}\})$ plotted on the same set of axes. From the vertical intercepts, the singularity location can be accurately estimated as $\epsilon^* = 0{\cdot}344 + i0{\cdot}237$. The horizontal intercept of each asymptote is almost certainly $n^{-1} = \frac{2}{3}$ which gives $\alpha = \frac{1}{2} + i0$ in equation (3.4*b*).

Similar plots have been made for a number of points on the free surface at $t = 0$. The locus of values $\epsilon^*(\xi)$, constructed from the results of these plots, is shown in figure 5. We note first that the curve has the property that $\mathrm{Re}\{\epsilon\}$ and $\mathrm{Im}\{\epsilon\}$ axes are lines of symmetry in the sense that $\epsilon^*(-\xi) = \overline{\epsilon^*}(\xi) = -\epsilon^*(\pi - \xi)$. This property follows readily from (2.12*a*) and (3·4*b*) so long as α is real. Along the solid curve in the figure, the ratio plots were unambiguous and clearly indicated a square-root singularity $\alpha = \frac{1}{2}$ at the indicated value of ϵ^*. Two points are also shown that were calculated for very small values of ξ corresponding to points near the crest on the wave profile. The ratio plots for these points were not sufficiently well structured to even estimate the nature of the singularity; thus it may or may not be a square root. The plots do however indicate a value of $\mathrm{Re}\{\epsilon^*\}$ of about 0·64, implying that the maximum amplitude/wavelength ratio, $\epsilon_{\max}/\pi$, for the standing wave in deep water is 0·204. The dotted lines in the figure represent a guess concerning the singularity structure of the ϵ expansion for $|\xi|$ very small. We suspect that there are two (or more) singularities in close proximity to one another, thus explaining the failure of the ratio plots to yield a well-defined asymptote. The nature of the limiting singularity for $|\xi|$ small is an important question; this knowledge would enable one to state conclusively whether the crest is pointed and, if so, would specify the included angle.

It is worthwhile to note in passing that those points lying on the solid line in figure 5 whose series expansions have singularities at strictly complex values of ϵ must also have a second singularity at the real value $\epsilon_{\max}$. Otherwise, it would be possible to compute values of z for $\epsilon > \epsilon_{\max}$ by a method of analytic continuation. It might be possible to extract information about this second singularity by 'mapping away' the leading singularity.

While the complex-valued singularities indicated in figure 5 are 'non-physical', they do define the radii of convergence of the ϵ expansions. Thus one can state quite unequivocally that the ϵ expansion of the wave profile function at $t = 0$

$$z(\xi, 0; \epsilon) = \sum_{n=0} z_n(\xi, 0)\, \epsilon^n$$

is not *uniformly* convergent for ϵ greater than 0·30. Thus wave profiles for ϵ greater than this critical value cannot be found by summing the series regardless of how many terms are known. It is necessary therefore to introduce a method of analytic continuation; we will use rational fractions (Padé approximants) for this purpose.

We will give a short heuristic motivation for their use; there is, of course, a substantial and rapidly growing body of literature on both the theory and application of Padé approximants (see Cabannes 1976). If only the first $2N+1$ coefficients are known for some function

$$f(\epsilon) = a_0 + a_1\epsilon + \ldots + a_{2N}\epsilon^{2N} + \ldots, \quad N = 1, 2, \ldots, \tag{3.10a}$$

the function f may be equally well approximated by an $[N/N]$ Padé approximant of the form

$$[N/N]f(\epsilon) = \frac{b_0 + b_1\epsilon + \ldots + b_N\epsilon^N}{1 + c_1\epsilon + \ldots + c_N\epsilon^N}, \tag{3.10b}$$

N	$\epsilon = 0{\cdot}40$		$\epsilon = 0{\cdot}50$		$\epsilon = 0{\cdot}60$		$\epsilon = 0{\cdot}65$	
1	$0{\cdot}5776 + i0{\cdot}4081$		$0{\cdot}6914 + i0{\cdot}5062$		$0{\cdot}8286 + i0{\cdot}5927$		$0{\cdot}9059 + i0{\cdot}6294$	
2	0·5988	0·3244	0·7101	0·3000	0·7920	0·1696	0·8036	0·6219
3	0·5756	0·3457	0·6841	0·4017	0·8343	0·4119	0·9191	0·3890
4	0·5779	0·3337	0·6542	0·3623	0·7185	0·3757	0·7487	0·3780
5	0·5779	0·3343	0·6566	0·3647	0·7286	0·3778	0·7665	0·3769
6	0·5779	0·3342	0·6556	0·3645	0·7267	0·3796	0·7628	0·3810
7	0·5800	0·3339	0·6536	0·3619	0·7115	0·3795	0·7374	0·3904
8	0·5800	0·3339	0·6541	0·3621	0·7150	0·3762	0·7416	0·3804
9	0·5800	0·3339	0·6539	0·3619	0·7125	0·3775	0·7376	0·3862
10	0·5800	0·3339	0·6538	0·3618	0·7108	0·3786	0·7351	0·3908

TABLE 3. Padé approximants $[N/N]\,z$ for $\xi = 0{\cdot}3242$ and $t = 0$.

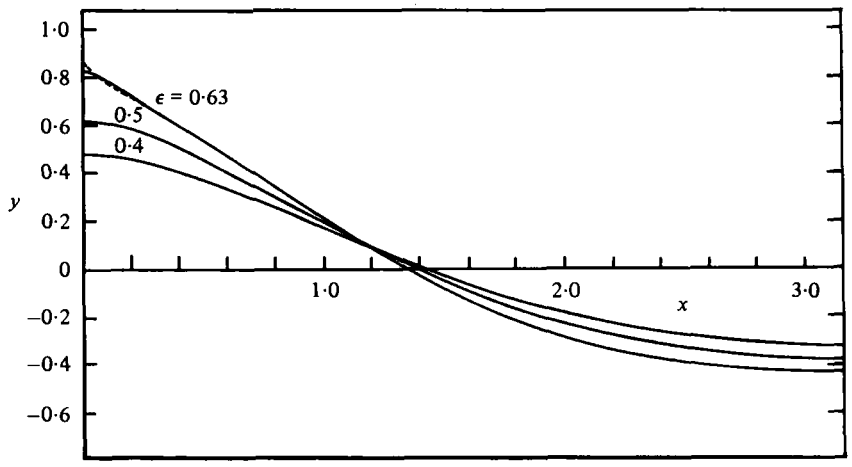

FIGURE 6. Surface profiles at $t = 0$ from [12/12] approximants.

where the b_j and c_j are determined uniquely ('pathological' cases excepted) from the a_j by expanding (3.10*b*) about $\epsilon = 0$ and equating the resultant power series with (3.10*a*) on a term-by-term basis. The error of the polynomial and the fractional forms are formally of the same order; the series, however, will only converge if ϵ lies within a circle whose radius is defined by $|\epsilon^*|$, the magnitude of the 'closest' singular point. The sequence of approximants $[N/N]f$, $N = 1, 2, \ldots$, will converge to f in a much larger domain, in general, and will fail to converge (in practice) only near branch points and resulting branch cuts of f. Rigorous proofs have been derived for certain classes of functions.

Table 3 shows the convergence of the approximants $[N/N]\,z(\epsilon)$ for our representative surface point corresponding to $\xi = 0{\cdot}3242$ and $t = 0$. The values of ϵ displayed are 0·4, 0·5, 0·6, and 0·65. From figure 4 we known that the radius of convergence for $\xi = 0{\cdot}3242$ corresponds to $\epsilon = |0{\cdot}344 + i0{\cdot}237| = 0{\cdot}418$, so the power series will converge slowly for $\epsilon = 0{\cdot}4$ and not at all for the other values. At the highest order considered in the table, convergence is at least four places for $\epsilon = 0{\cdot}4$ and about one part in 4000 for $\epsilon = 0{\cdot}5$. For $\epsilon = 0{\cdot}6$, the tables converge to perhaps one part in 300 and about one part in 100

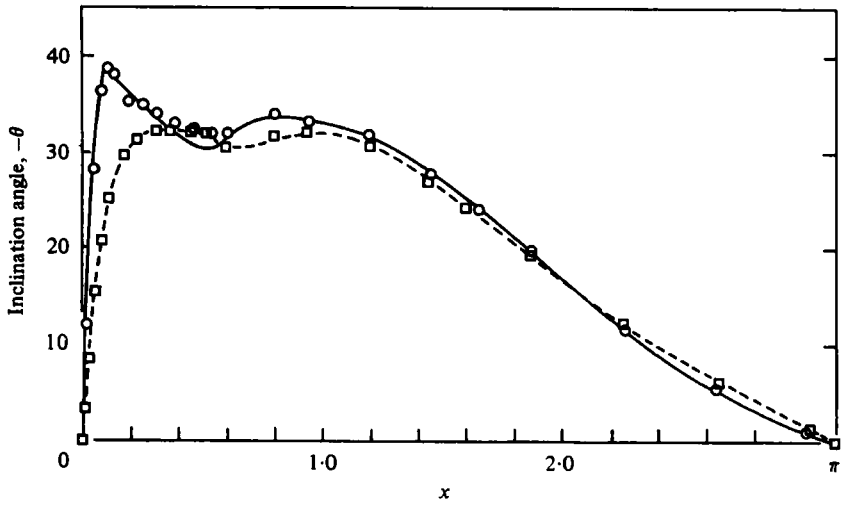

FIGURE 7. Surface inclination at $t = 0$. For $\epsilon = 0{\cdot}60$: □, [10/10]; – – –, [12, 12]. For $\epsilon = 0{\cdot}63$: ○, [10/10];——, [12, 12].

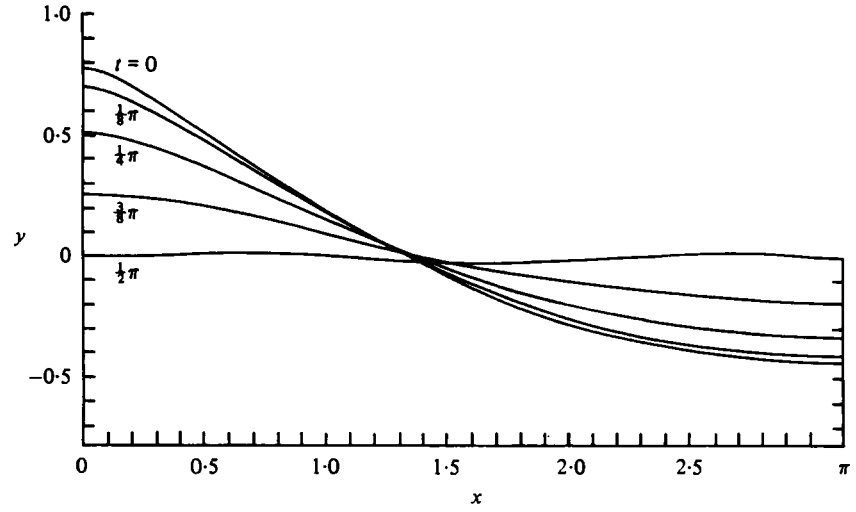

FIGURE 8. Surface profiles *versus* time, $\epsilon = 0{\cdot}60$.

for $\epsilon = 0{\cdot}65$. In light of the estimate made above for $\epsilon_{\max}$, the $\epsilon = 0{\cdot}65$ tables may not be convergent at all.

Similar tables were computed for many values of ξ to produce $t = 0$ wave profiles for several values of ϵ. On average, the convergence was slightly better than that of table 3. Figure 6 shows three surface profiles corresponding to $\epsilon = 0{\cdot}4$, $0{\cdot}5$, $0{\cdot}63$. For the $\epsilon = 0{\cdot}63$ case, the profile shown was drawn from the [12/12] approximants. Lower-order fractions agreed, in general, to about 1 % for y at a given value of x. For the cases corresponding to smaller values of ϵ, the tables converged to at least graphical accuracy. The highest surface profile in the figure has an interesting property. It has three inflexion points rather than one. This is illustrated more clearly in figure 7 which

shows the surface inclination for the $\epsilon = 0{\cdot}6$ and $0{\cdot}63$ profiles. In the former case, the magnitude of the inclination attains its maximum value $\theta_{\max} = 32{\cdot}2°$, at $x \simeq 0{\cdot}33$. There is a second maximum with $\theta = 32{\cdot}0°$ at $x \simeq 1{\cdot}00$. The dashed curve is drawn from the [12/12] approximant for $z_\xi = x_\xi + iy_\xi$. The [10/10] approximant is also shown and it may be seen that the two are in close agreement. For $\epsilon = 0{\cdot}63$, both the [10/10] and [12/12] approximants indicate $\theta_{\max}$ is about 39°, occurring at $x \simeq 0{\cdot}10$. While the two approximants do not agree on the magnitude of the intervening minimum, they each predict a second maximum at $x \simeq 0{\cdot}80$.

Figure 8 shows the free surface shape for $\epsilon = 0{\cdot}60$ at various times from $t = 0$ to $t = \frac{1}{2}\pi$, the quarter-period value. Notice that the surface is not flat at $t = \frac{1}{2}\pi$, the maximum displacement being about $0{\cdot}004\lambda$ at $x = \frac{1}{2}\pi$. For $\frac{1}{2}\pi < t < \pi$, the profiles will be left–right reflexions of those shown and, for $\pi < t < 2\pi$, the surface will merely assume the profiles shown, but in reverse order. The shape of the nearly flat profile, at $t = \frac{1}{2}\pi$, is not well represented by the equation (3.3), which is not surprising in view of the relatively large value of ϵ.

In figure 6 we show a plausible highest wave exhibiting a 45° inclination and a sharp crest. While the argument of Penney & Price, indicating a crest with a 90° included angle, may be defective,† the curves in figure 6 suggest that this local behaviour is quite probable. With the additional assumption that the profile will change very little except near the crest as the value of $\epsilon_{\max}$ is approached, we have indicated a slight modification, corresponding to a plausible highest wave, by the dashed curve. The curve was drawn so as to conserve mass between it and the $\epsilon = 0{\cdot}63$ profile. This possible highest wave has $\epsilon_{\max} \simeq 0{\cdot}65$, corresponding to a wave-height/length ratio of $0{\cdot}207$.

Penney & Price argue that the deceleration at the crest cannot exceed g in magnitude. The premise of their argument is that a fluid element 'cannot withstand tension'; hence $p \geqslant 0$ within the fluid. While this is undoubtedly correct, it is possible to demonstrate this fact without appealing to physical intuition. From equation (2.5) we observe that p satisfies Laplace's equation at $t = 0$ when the fluid is instantaneously at rest. On the free surface we have $p = 0$, while some distance below the surface the pressure differs little from the hydrostatic value, a positive quantity. A function that satisfies Laplace's equation will not admit an interior extremum; it follows therefore that $p \geqslant 0$ within the fluid at $t = 0$. Since $p = 0$ on the surface, it follows that

$$\mathbf{n}.\nabla p \leqslant 0 \quad \text{on} \quad \eta = 0 \quad \text{at} \quad t = 0, \tag{3.11}$$

where $\mathbf{n}$ is an outward normal vector. At the crest, $x = 0$, (3.11) is equivalent to $\partial p/\partial y \leqslant 0$. The vertical component of the Euler equation

$$\frac{\partial \mathbf{v}}{\partial t} + (\mathbf{v}.\nabla)\,\mathbf{v} = -g\mathbf{j} - \frac{1}{p}\nabla p, \tag{3.12}$$

† Their prediction assumes that the pressure p is regular in a neighbourhood of the sharp crest and can thus be expanded in a Taylor series about this point. Then, by invoking symmetry and the fact that p satisfies Laplace's equation at those instants of time when the fluid is at rest, they show that the two sides are each inclined at 45° to the vertical. There would not appear to be any compelling reason for accepting that the sharp crest is a regular point for p. Surely p is singular at some points in the physical half-plane lying above the fluid; it is plausible that one or more of these singularities will move down to meet the sharp crest as the highest wave is approached.

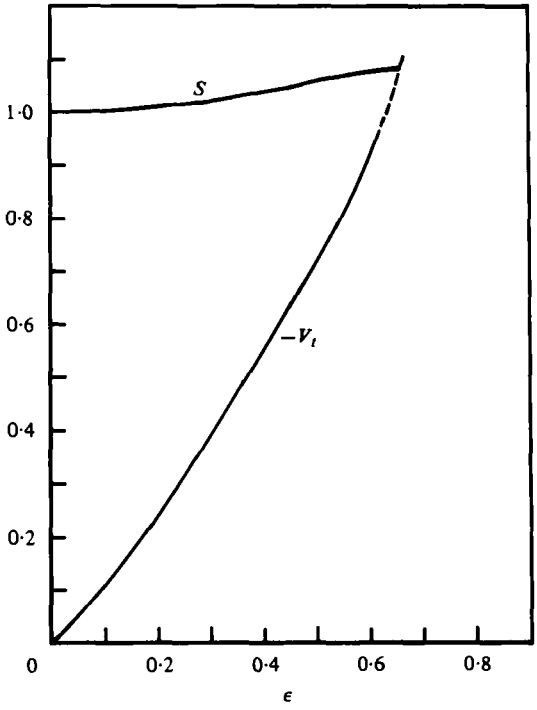

FIGURE 9. Crest deceleration at $t = 0$ and frequency parameter *versus* wave height.

when evaluated at $t = 0$, gives the inequality

$$\frac{\partial v}{\partial t} + g \geqslant 0 \quad \text{at} \quad t = 0 \tag{3.13}$$

at the crest, thereby agreeing with Penney & Price.

In the dimensionless units of § 2, (3.13) can be written in ζ-plane variables as

$$V_t + S \geqslant 0 \quad \text{at} \quad t = 0 \quad \text{and} \quad \xi = 0, \tag{3.14}$$

where S is the frequency parameter given by equation (2.10). The criterion (3.14) can be used to estimate $\epsilon_{\max}$. Figure 9 shows the Padé-summed results of the ϵ series for the crest deceleration and the frequency parameter S plotted as functions of ϵ. The approximants converged well up to $\epsilon = 0{\cdot}62$ for both curves. For larger values of ϵ, the highest-order approximant available was used. The intersection of the two curves gives a value of $\epsilon_{\max}$ between 0·66 and 0·67, essentially consistent with earlier estimates. Thus we feel that a value

$$\left.\frac{A}{\lambda}\right|_{\max} = 0{\cdot}208$$

should be accurate to within 3 %.

No strong argument, other than numerical extrapolation, can be given for a 90° crest angle, however. For $\epsilon \geqslant 0{\cdot}5$ and $t = 0$ we have a sufficient number of terms in our solution to determine about ten coefficients $a_j(\epsilon)$ in the expansion

$$z = \zeta + i \Sigma a_j e^{-ij\zeta}$$

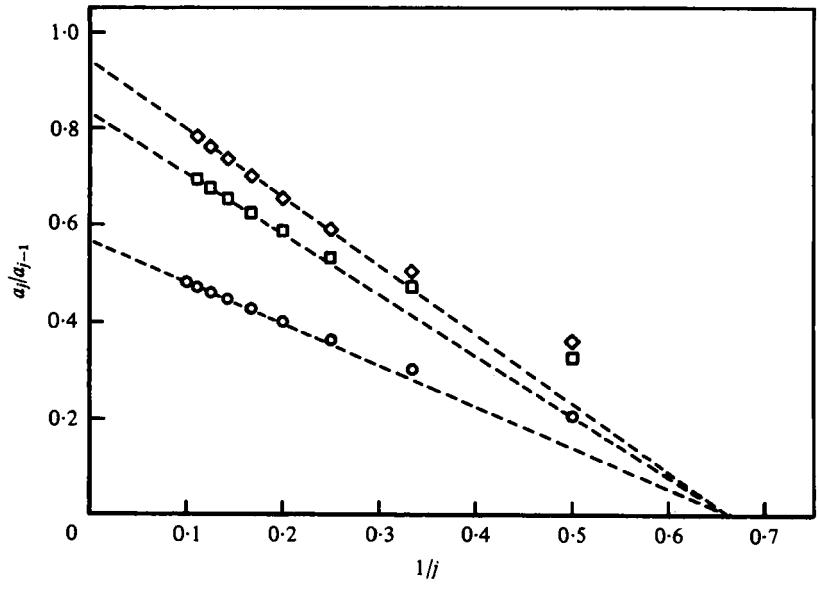

FIGURE 10. Domb–Sykes plots for a_j/a_{j-1} at $t = 0$.
○, $\epsilon = 0{\cdot}224$; □, $\epsilon = 0{\cdot}387$; ◇, $\epsilon = 0{\cdot}500$.

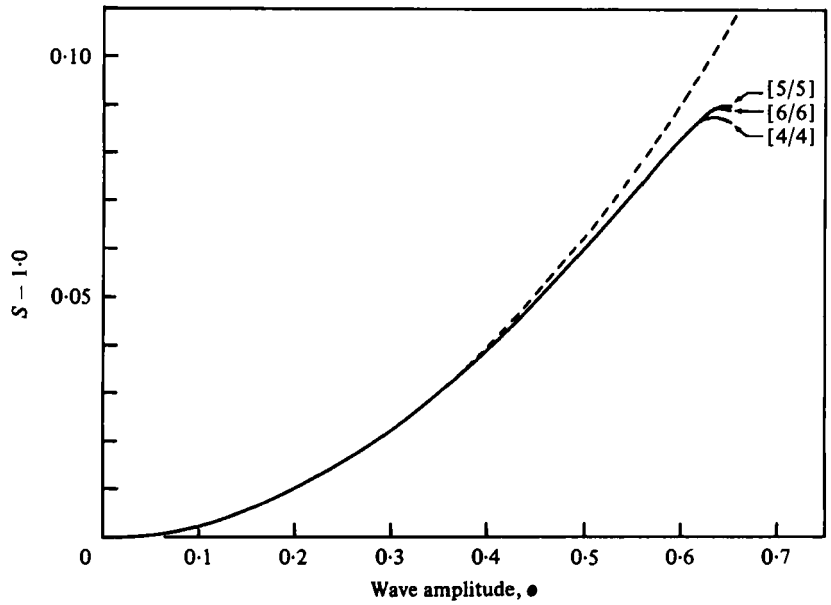

FIGURE 11. Frequency parameter *versus* wave height; – – –, $\frac{1}{2}\epsilon^2$.

by computing the a_j as converged approximants for specified values of ϵ. Ratio plots for various values of ϵ are shown in figure 10. They indicate a square-root singularity at values of $e^{-i\zeta}$ which tend to 1 as ϵ is increased. If we assume that a square-root singularity also exists for $e^{-i\zeta} = 1$ or $\zeta = 0$ at $\epsilon = \epsilon_{\max}$, then

$$z \sim i(1 - e^{-i\zeta})^{\frac{1}{2}} \sim i(i\zeta)^{\frac{1}{2}},$$

which readily gives

$$\arg_{\xi\to 0^+}(z) = -\frac{\pi}{4}, \quad \arg_{\xi\to 0^-}(z) = +\frac{\pi}{4},$$

thus exhibiting the 90° crest. While we believe this to be correct, we note that exactly the same situation occurs for the progressive wave, i.e. a $\frac{1}{2}$-power singularity is indicated for waves of less than maximum height. The required $\frac{1}{3}$-power singularity corresponding to the 120° crest angle is explained by Grant (1973*a*) as arising from the coalescence of two square-root-type singularities.

Figure 11 shows the frequency parameter, calculated from (3.2) by $[N/N]$ approximants, plotted *versus* wave height. The approximants converge to graphical accuracy to about $\epsilon = 0{\cdot}62$. S appears to attain a maximum value of 1·089 near $\epsilon = \epsilon_{\max}$. It has recently been shown (Longuet-Higgins & Fox 1978; Schwartz & Vanden-Broeck 1979) that the wave speed for steady *progressive* waves achieves a succession of maximum and minimum values as the highest wave is approached. It is possible that S exhibits similar behaviour in the present problem. Note that the linear approximation to the period of a standing wave in deep water

$$T_0 = \left(\frac{2\pi\lambda}{g}\right)^{\frac{1}{2}}$$

is never in error by more than 4·4%. The two-term approximation, $S = 1 + \frac{1}{4}\epsilon^2$, is shown for comparison in the figure.

Since most of the quantities considered were computed by high-order rational fractions, a partially independent check can be made by verifying that equations (2.3), (2.4) and (2.6) are satisfied for various values of ξ, t, and ϵ. Each quantity appearing in these equations was evaluated as a rational fraction for several values of ϵ at $t = 0$ and $t = \frac{1}{4}\pi$. Typically, [10/10] or [12/12] fractions satisfied the equations to one part in 10^7, 600, and 300, for $\epsilon = 0{\cdot}4$, 0·6, and 0·62, respectively. These numbers are consistent with the degree of convergence of the $[N/N]$ approximants themselves.

4. Concluding remarks

An algorithm has been developed for the series solution of time- and space-periodic standing waves. By use of a time-dependent conformal map, the problem may be solved in a fixed region in the transformed plane. This results in a substantial simplification in the algebraic manipulations and makes automatic computation feasible.

The solution has the property that nth-degree Fourier components of the time and space dependence first appear at nth order in the wave amplitude. Thus, as the amplitude goes to zero, the solution is simply periodic in space and time. This structure is analogous to that assumed by Stokes (Stokes's hypothesis) for steady progressive waves. The possible existence of other families of standing waves with more complicated structure at leading order in the amplitude has not been excluded, however.†

† A significant discussion on this point has occurred during the review process for this paper. Unlike the steady progressive wave, the periodic standing wave formally allows superposition of higher harmonics at leading order. Thus, to the right side of equation (2.16), a linear combination of terms of form $\epsilon a_n \cos n^2 x \cos nt$, $n = 2, 3, \ldots$, can be appended. It is our belief, however, that the resonance-suppression requirement will force each a_n to be zero. For example, if a_2 is taken to be arbitrary initially with $a_n = 0$, $n > 2$, it can be shown that a_2 must also be zero for, if it were not, a secular term would be forced at $O(\epsilon^3)$.

A vital feature of the standing-wave problem is the need to suppress secular terms in the time dependence. Such terms would result from incorrect choices of the 'homogeneous' solutions when p, the index of the space variation, is a perfect square. By looking ahead to higher order in the amplitude, the correct value of the constants can be found. The procedure is similar, for example, to the 'method of strained coordinates' as applied to the series solution for the nonlinear pendulum. The representation of the solution has been shown to be adequate in the sense that secular terms can always be suppressed when the index n, defined in (2.17), is greater than zero. When n equals zero we have demonstrated that secular terms cannot appear provided $p \leqslant 81$. No doubt an inductive proof can be devised, by examining the recurrence equations, to exclude secular terms, for any p, when $n = 0$. More importantly, our high-order series results strongly indicate convergence and hence existence of time- and space-periodic standing waves for sufficiently small amplitude. For a rigorous proof of existence it would be sufficient to establish upper bounds on the series coefficients by manipulating the recurrence equations. The results presented in figure 5 indicate that the series solution for the wave profile is uniformly convergent when the highest parameter ϵ is less than about 0·30. For greater values the series will not converge everywhere in the half-plane $\mathrm{Im}\,\zeta \leqslant 0$, but the series in ϵ can be summed by the use of Padé approximants.

We have verified the result of Penney & Price (1952) that at no instant of time is the surface ever flat and hence that the nonlinear standing wave does not possess any true nodes. The deviation from a horizontal surface is, as they predict, fourth order in the amplitude but the shape they propose would not appear to be correct.

The shape of the free surface when the fluid is at rest, for waves close to the highest, is more complicated than had been previously assumed. In particular for such waves we have found *two* local maxima of surface slope. It is possible that more undulations will appear for still higher waves.

In an attempt to predict the maximum wave steepness, three different extrapolations were used. Apparently because the singularity structure near the crest of the highest wave is quite complicated, the three predictions agreed only moderately well and suggest a value of amplitude/wavelength between 0·204 and 0·213. The experiments of Taylor indicate a result about 10 % higher than this. The discrepancy may be due to the surface tension of the real fluid. We note that surface forces could be included in the present analysis without very great additional difficulty; it would then no longer be possible for an ideally sharp crest to form and the maximum wave probably would be topologically limited as is the corresponding progressive wave.

For waves somewhat short of the highest, we find a square-root singularity for the wave profile series lying above the fluid region in the ζ plane. This singularity moves down towards the crest as the amplitude increases. Its presence suggests that the limiting wave most likely has a right-angled crest as predicted by Penney & Price; however, we feel that the evidence is less than conclusive.

The bulk of this work was completed while L.W.S. was a Visiting Research Fellow in the Department of Naval Architecture at the Berkeley campus of the University of California. He would like to acknowledge their hospitality and thank, in particular, Professor John Wehausen for a number of useful discussions. The work of A.K.W. was supported, in part, by the Lockheed Independent Research Program.

Appendix. On the structure of the 'first column' solution

Grant (1973*b*) gives a system of partial differential equations which is equivalent to (2.18) with $n = 0$. If we let

$$\mathscr{F} = \sum_{p=1} \alpha_{p0} \chi^p$$

and

$$\mathscr{G} = \sum_{p=1} \gamma_{p0} \chi^p,$$

where $\chi = \epsilon e^{-i\zeta}$, Grant's equations can be written as

$$\frac{\partial \mathscr{F}}{\partial t} = \chi \frac{\partial \mathscr{G}}{\partial \chi}, \tag{A 1a}$$

$$\left(1 + \chi \frac{\partial \mathscr{F}}{\partial \chi}\right)\left(\frac{\partial \mathscr{G}}{\partial t} + \mathscr{F}\right) = \left(\frac{\partial \mathscr{F}}{\partial t}\right)^2. \tag{A 1b}$$

These equations can be shown to have a class of exact solutions. We assume a solution of the form

$$\mathscr{F} = H(\mu_k), \quad \mathscr{G} = -\frac{1}{k^{\frac{1}{2}}} \tan k^{\frac{1}{2}} t H(\mu_k)$$

where $\mu_k = A_k \chi^k \cos k^{\frac{1}{2}} t$ and the constants A_k are initially free. Equation (A 1*a*) is satisfied identically while (A 1*b*) yields an equation for $H(\mu_k)$ of the form

$$\mu_k H' - H - k\mu_k H H' = 0,$$

with the exact solution

$$\mu_k = H e^{-kH}. \tag{A 2}$$

Here the constant of integration has been absorbed in A_k. A series representation for $H(\mu_k)$ and hence for $\mathscr{F}(\chi, t)$ can be obtained from (A 2) by use of Lagrange's formula (see Whittaker & Watson 1927). We obtain

$$\mathscr{F}(\chi, t; k, A_k) = \sum_{p=1}^{\infty} \frac{(kp)^{p-1}}{p!} A_k^p \chi^{kp} \cos^p k^{\frac{1}{2}} t. \tag{A 3}$$

The solution for $\mathscr{F}$ obtained by Grant is (A 3) with $k = A_k = 1$. He obtains simply

$$\alpha_{p0} = \frac{p^{p-1}}{p!} \cos^p t.$$

Grant's solution fails to suppress resonance in the second column, however, starting with his value of $\alpha_{401} = \frac{4}{3}$ which must be replaced by $\frac{65}{48}$.

The only permissible values of k in (A 3) are perfect squares for the usual reason. Inspection of the computed solution for α_{p0} reveals that, at least through $p = 8$, $\mathscr{F}$ can be expressed as a multiple power series of the form

$$\mathscr{F} = \sum_{i,j,k,\ldots} C_{ijk} \mu_1^i \mu_4^j \mu_9^k \ldots. \tag{A 4}$$

Based on this observation and the preceding discussion, we are led to formulate the following unproven conjecture:

An analytic function $\mathscr{F}$ *of the variables* $\mu_1, \mu_4, \ldots, \mu_{I^2}$ *can be found which satisfies* (A 1) *and hence* (2.18) *with* $n = 0$. *That is*

$$\mathscr{F} = \mathscr{F}(A_1 \chi \cos t, A_4 \chi^4 \cos 2t, \ldots, A_{I^2} \chi^{I^2} \cos It),$$

where I *is any positive integer and the* A_{j^2} *are real constants. If all but one of the* A*'s are zero, the functional form of* $\mathscr{F}$ *is given by* (A 3).

The values of the A's for the standing-wave expansion will be those that suppress resonance. In particular, $A_1 = 1$ from the definition of ϵ and $A_4 = \frac{1}{48}$.

REFERENCES

Cabannes, H. 1976 *Padé Approximants Method and its Application to Mechanics*. Springer.

Chabert-D'Hières, G. 1960 *Houille Blanche* **2**, 153–163.

Domb, C. & Sykes, M. F. 1957 *Proc. Roy. Soc.* A **240**, 214–228.

Edge, R. D. & Walters, G. 1964 *J. Geophys. Res.* **69**, 1674–1675.

Fultz, D. 1962 *J. Fluid Mech.* **13**, 193–212.

Grant, M. A. 1973*a* *J. Fluid Mech.* **59**, 257–262.

Grant, M. A. 1973*b* *J. Fluid Mech.* **60**, 593–604.

Longuet-Higgins, M. S. & Fox, M. J. H. 1978 *J. Fluid Mech.* **85**, 769–786.

Penney, W. G. & Price, A. T. 1952 *Phil. Trans. Roy. Soc.* A **244**, 254–284.

Rayleigh, J. W. S. 1915 *Proc. Roy. Soc.* A **91**, 345–353.

Saffman, P. G. & Yuen, H. C. 1979 *J. Fluid Mech.* **95**, 707–715.

Schwartz, L. W. 1974 *J. Fluid Mech.* **62**, 553–578.

Schwartz, L. W. & Vanden-Broeck, J. M. 1979 *J. Fluid Mech.* **95**, 119–140.

Schwartz, L. W. & Whitney, A. K. 1977 *6th Australasian Hydraulics and Fluid Mech. Conf.* Preprints of Papers Part I, pp. 356–359.

Sekerzh-Zen'kovich, Ya. I. 1947 *Dokl. Akad. Nauk S.S.S.R.* **58**, 551–553.

Stokes, G. G. 1880 *Mathematical and Physical Papers*, vol. 1. Cambridge University Press.

Tadjbakhsh, I. & Keller, J. B. 1960 *J. Fluid Mech.* **8**, 442–451.

Taylor, G. I. 1953 *Proc. Roy. Soc.* A **218**, 44–59.

Wehausen, J. V. 1965 In *Research Frontiers in Fluid Dynamics* (ed. R. J. Seeger & G. Temple), p. 534. Wiley Interscience.

Wehausen, J. V. & Laitone, E. V. 1960 In *Handbuch der Physik*, vol. 9 (ed. S. Flügge), p. 446. Springer.

Whitney, A. K. 1971 *Proc. 2nd Int. Conf. on Numerical Methods in Fluid Dynamics* (ed. M. Holt), p. 458. Springer.

Whittaker, E. T. & Watson, G. N. 1927 *A Course in Modern Analysis*, 4th edn. Cambridge University Press.